

# EXPERIMENTAL INVESTIGATION ON THE SECONDARY MOTION DOWNSTREAM A PIPE BEND WITH AND WITHOUT SWIRL

*A. Kalpakli and R. Örlü*

*CCGEx & Linné FLOW Centre, KTH Mechanics, SE-100 44 Stockholm, Sweden*

[ramis@mech.kth.se](mailto:ramis@mech.kth.se)

## Abstract

The turbulent swirling flow at the exit of a 90 degree pipe bend, generated through an axially rotating pipe upstream the bend, is investigated by means of time-resolved stereoscopic particle image velocimetry. In particular, the behavior of the Dean vortices under turbulent flow conditions, the so called “swirl switching”, has been visualized with the aid of proper orthogonal decomposition. This phenomenon could be reconstructed by only a few of the most energetic modes. With the increase of the swirl number, defined as the azimuthal velocity of the rotating pipe upstream the pipe bend to the bulk velocity, the two Dean cells tend to merge for a swirl number close to unity. Vortical cells, similar to the Dean vortices, are found beneath the primary swirling motion, and are captured in the first mode of the decomposed field. The present investigation constitutes—to the authors’ knowledge—the first experimental study of the three velocity components in a swirling turbulent pipe flow across the exit of a pipe bend.

## 1 Introduction

Laminar flow through pipe bends has been investigated for decades, theoretically (Dean 1927), numerically (McConalogue and Srivastana 1968) and experimentally (Eustice 1911) due to the occurrence of curved geometries in natural and biological systems. It is known that under the effect of curvature, the high speed fluid is deflected towards the outer wall while the slow moving fluid flows towards the inner pipe side, thereby constituting the steady *Dean vortices*. Under turbulent flow conditions, Tunstall and Harvey (1968) have shown that the Dean vortices are highly unsteady and depict a dominating vortex oscillating in clockwise and counter-clockwise directions. This phenomenon, known in the literature as “swirl switching” (Brücker 1998, Rütten et al. 2005), is still attracting scientific attention (Sakakibara and Machida 2012) and has been identified as a possible source of fatigue in piping systems.

The case of turbulent flow through pipe bends when an additional swirling motion is added to the primary flow, has—despite its industrial relevance—only been investigated to a limited extent both from a numerical (Pruvost et al 2004) and experimental (Anwer and So 1993) point of view. In particular, there is a clear lack of information on the interaction between the swirling motion and the Dean vortices under turbulent flow conditions, since previous experimental investigations were limited to point-wise measurements.

In the present work, the three-dimensional flow field under turbulent flow conditions downstream a 90 degree pipe bend has been captured by means of Time-resolved Stereoscopic Particle Image Velocimetry (TS-PIV). The secondary structures were visualized and quantified for a non-swirling and swirling flow of varying intensity, up to the condition where the motion is swirl dominated. A phenomenon similar to the “swirl switching” as well as the existence of the Dean vortices in a turbulent swirling flow were investigated through post-processing of the PIV data by means of *snapshot* Proper Orthogonal Decomposition (POD) (Sirovich 1987).

## 2 Experimental set-up and measurement technique

The measurements for the current study were conducted at the *Fluid Physics Laboratory* at *KTH Mechanics* within the *rotating pipe facility* depicted in figure 1b) with air as working fluid. The facility consists of a circular pipe that can rotate up to 2000 rpm by means of DC motor. The total length of the rotating pipe section is  $100 D$  where  $D$  denotes the inner diameter of the pipe, equal to 60 mm. The fully developed turbulent pipe flow established at the downstream end of the pipe, documented in e.g. Sattarzadeh (2011), constitutes also the inflow condition for the flow into the bent pipe (figure 1a). Note that while the straight pipe is rotating, the bend is remaining still. The curved pipe has a curvature centerline radius of  $R_c = 95.3$  mm, giving a curvature ratio  $R/R_c$  of 0.31. The length of the straight section after the 90°

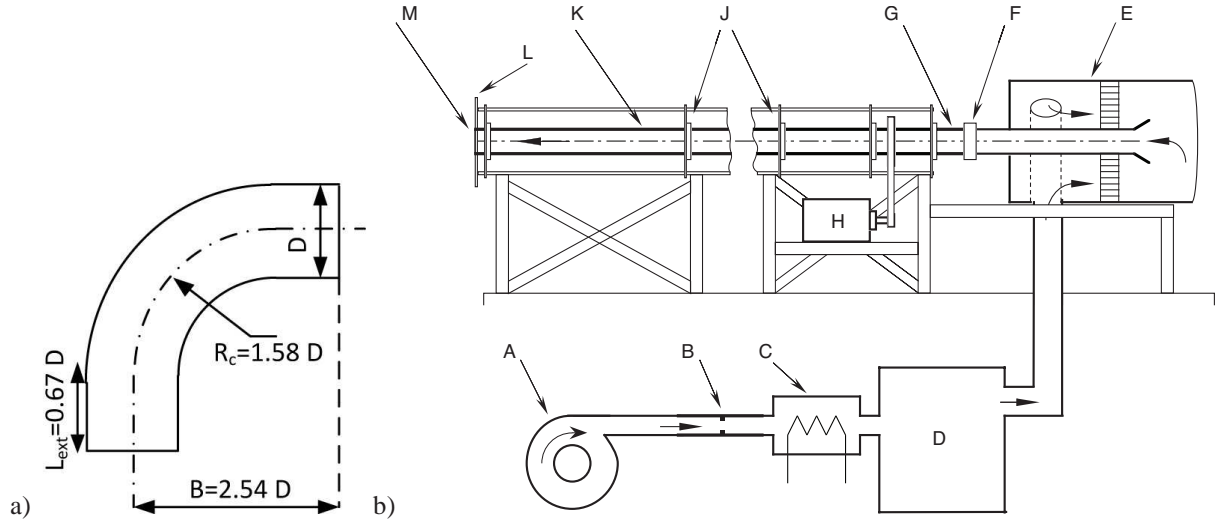


Figure 1: *a)* Dimensional details of the 90° pipe bend. *b)* Schematic of the experimental set up. **A)** Centrifugal fan, **B)** flow meter, **C)** electrical heater, **D)** distribution chamber, **E)** stagnation chamber, **F)** coupling between stationary and rotating pipe, **G)** honeycomb, **H)** DC motor, **J)** ball bearings, **K)** rotating pipe, **L)** circular end plate, **M)** pipe outlet to which the pipe bend (shown to the left) has been mounted.

Table 1: Parameter range for the experiments.

$Re \times 10^{-3}$	$De \times 10^{-3}$	$S$
14	8	0.85, 1.2
24	13	0.1, 0.3, 0.5
34	19	0

curvature is  $0.67 D$ . For a fully developed axially rotating straight pipe flow the swirling flow can fully be characterized by means of the Reynolds number,  $Re_D$  (here defined through the bulk velocity  $W_b$  and pipe diameter  $D$ ) and swirl number  $S$  defined as the ratio of azimuthal velocity of the pipe wall  $U_w$  to bulk velocity. For flows through bends an additional parameter becomes important, namely the Dean number defined as:  $De = Re_D \times \sqrt{R/R_c}$ . The parameter range investigated in the present study is listed in table 1.

Time-resolved stereoscopic PIV has been employed in the present investigation to capture all three velocity components at the exit of the pipe bend. Two high-speed C-MOS cameras (Fastcam APX RS, Photron, 3000 fps at  $1024 \times 1024$  pixels) were positioned at an angle of approximately  $90^\circ$  and at forward-backward scatter mode at the exit of the pipe bend (around  $0.5$  mm from the exit). The two 105 mm Nikon Nikkor lenses were adjusted using a Scheimpflug adapter. A laser light sheet of approxi-

mately 1 mm thickness was produced by a Nd-YLF laser (Pegasus, 10 kHz maximum frequency, New Wave Research) and a water-based solution (Jem Pro Smoke Super ZR-Mix) was atomized using a high volume liquid seeding generator (10F03 Seeding Generator, DANTEC). For the *in-situ* calibration of the cameras, images were taken of a two-level calibration plate and the pinhole model was used in order to fit the dewarping mapping function to the marks found in each image, with the commercial software *DaVis 7.2* from *LaVision GmbH*. A self-calibration procedure has also been applied to eliminate errors from misalignment of the laser light sheet with the calibration target (Wieneke 2005). The post-processing of the PIV data was performed using *DaVis 7.2* and the vector fields were calculated through a multi-pass correlation iteration procedure in order to increase resolution, starting with a  $64 \times 64$  px interrogation window and decreasing to  $16 \times 16$  px interrogation window with 50 % area overlapping.

The raw images from the measurements had a resolution of  $1024 \times 1024$  px at 10-bit while the field of view was equal to  $80 \times 80$  mm<sup>2</sup> in physical space.  $N_s = 3000$  images were acquired for the non-swirling case at  $Re_D = 34 \times 10^3$  and 1000 images for the rest of the cases at a sampling frequency,  $f_s$ , of 1 kHz. It should be noted here that the aim of the present study is the characterization and identification of large scale structures under the effect of different flow conditions, and it is in this context that the term *time-resolved* is used, i.e. it implies that the most energetic structures are resolved in time.

### 3 Results

#### Dean vortices in turbulent flow

Since the focus of the present investigation is on the in-plane velocity components and the large-scale vortical structures, Reynolds number effects in the mean field within the investigated range of  $Re_D = 14 - 34 \times 10^3$  can safely be neglected (see e.g. Kalpakli 2012). Therefore, the following subsection will focus on results from TS-PIV measurements of a turbulent flow downstream a  $90^\circ$  pipe bend at  $Re_D = 34 \times 10^3$ , which is the highest achievable with the present experimental set up.

The time-averaged velocity field for the Reynolds number considered here is depicted in figure 2, with the streamwise velocity component plotted as the background contour map and the secondary motion, i.e. in-plane components, as streamlines. The formed flow field bears the characteristics of flows through pipe bends, i.e. the high velocity fluid is deflected towards the outer wall of the pipe (leftmost side) while the slower moving fluid flows towards the inner wall creating a C-shaped flow field, due to the interaction between centrifugal forces and a pressure gradient. This gives rise to the superposition of the Dean vortices on the primary field which are depicted clearly as two bean-shaped symmetrical cells. The highest in-plane velocity component here is 0.3 times the bulk velocity. The symmetry of the upper and lower Dean cells is a clear indication of both the quality of the set-up and converged statistics.

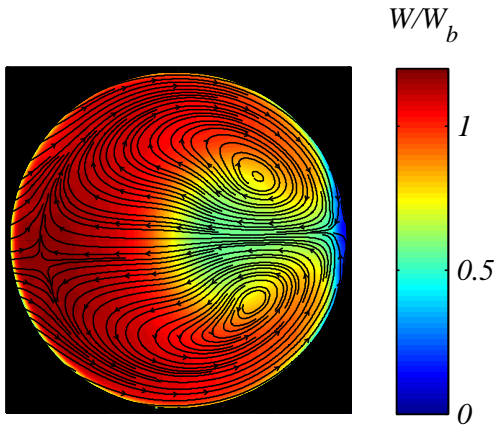


Figure 2: Time-averaged velocity field across a pipe cross-section for  $Re_D = 34 \times 10^3$ . The background contour map denotes the streamwise velocity component distribution scaled by the bulk speed and the in-plane components (largest mean value  $0.3 \times W_b$ ) are shown with the streamlines. The outer and inner pipe walls (in respect to the bend) correspond to the left and right side of the figure, respectively.

The unsteady behavior of the Dean vortices in a turbulent pipe bend flow has been illustrated in a previous study by the present authors (Kalpakli et al 2011). In the present work, an effort to reconstruct the phenomenon by means of snapshot POD is undertaken. The advantages that such kind of post-processing offers is that it can be used to suppress small scale fluctuations, and highlight periodicities in the behavior of the flow structures by reconstructing the flow field by the most energetic modes. Assuming that the Dean vortices are quite energetic, it is expected that decomposing the flow field and reconstructing it by using only the most energetic modes will reveal the vortical motion, filtering at the same time noise from the PIV data.

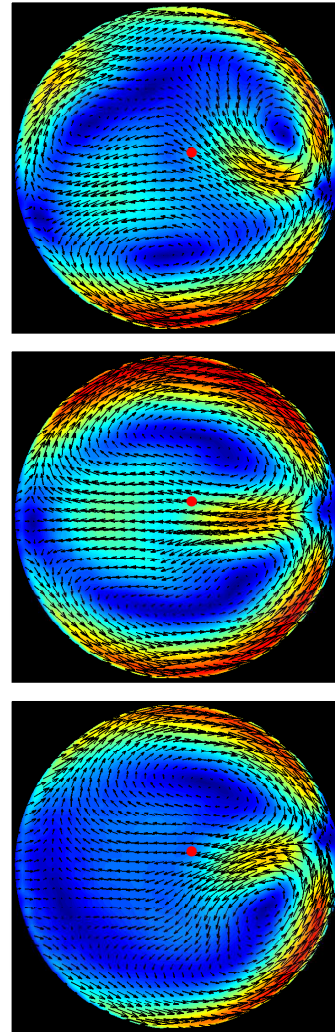


Figure 3: Reconstructed velocity field at three instants of time showing the magnitude of the in-plane components ( $\sqrt{U^2 + V^2}$ ) as contour map and their direction as vectors. The highest magnitude value (shown with red color) is  $0.5 \times W_b$ . The dot indicates the location  $x = 0.1R, y = 0.05R$  used for subsequent analysis.

The POD analysis for this task was performed on all  $N_s = 1500$  snapshots with a temporal resolution of  $\Delta t_s = 1/500$  s. Note that in the present analysis we concentrate on the vortical structures therefore the POD results are 2-D fields.

Figure 3 shows the 2-D field reconstructed by using only the first six modes which capture around 70% of the total energy. The unsteady motion of the vortices is clearly depicted interchanging between three states: a symmetrical one, where two vortices resemble the ones seen in the time-averaged field (figure 2), and two where one of the vortices dominates the cross-section and rotates in reference to the plane of symmetry either in the clockwise or anti-clockwise direction.

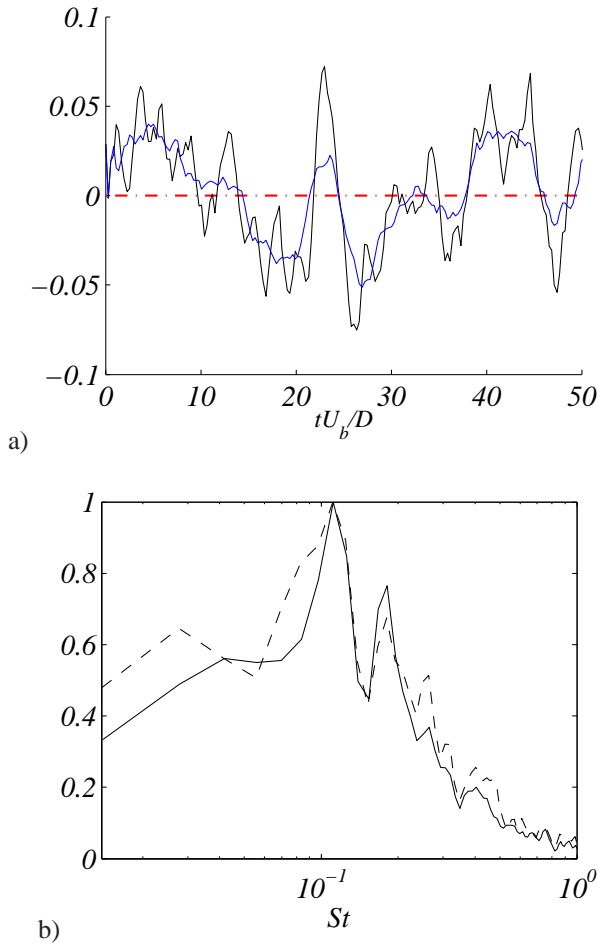


Figure 4: *a)* Time-series of the circumferential velocity component at  $x = 0.1R, y = 0.05R$ . Blue line denotes the low frequency variations (time-series smoothed with a moving average of 15). *b)* Power spectral density, scaled by the highest value, plotted against the Strouhal number. Reconstructed time series (solid line) as shown in (*a*) and 1st POD coefficient (dashed line).

In order to detect the frequency at which the vortices switch position, the flow field has been monitored in time in order to decide at which location the time-series should be investigated. The Power Spectral Density (PSD) of the circumferential velocity component was computed at  $x = 0.1R, y = 0.05R$  ( $R$  denoting the pipe radius), towards the inner wall and the result is shown in figure 4 along with the corresponding time series (which were smoothed by means of a moving average of degree 5 (black line) and 15 (blue line) to highlight the periodical behavior). The spectra was computed using Welch's method, by employing 10 windows with 50% overlap. A dominant peak at a Strouhal number  $St = fD/W_b = 0.11 \pm 0.01$  can be observed in the PSD for a number of loci at which the switching was identified by visual inspection. This value is also close to those reported in the literature (Brücker 1998, Sakakibara et al 2010).

In order to additionally examine and support the aforementioned observations on the swirl switching frequency and exploit the possibilities that POD offers, the spectra of the first POD coefficient has been computed and plotted together with the spectra from the reconstructed time series in figure 4; a procedure that was previously also adapted by Sakakibara et al (2010).

The spectra of the first chrono-mode not only agrees well with the spectra of the time-series but depicts additionally more clearly the low-frequency peak at  $St = 0.03$ . The spectra of the second and third POD coefficients have also been computed (not shown here) and for the second mode peaks at the same Strouhal numbers are found. This is explained due to the fact that the swirl switching is expected to be one of the most energetic features in the flow field, and should therefore be represented by the first modes.

### Swirling turbulent bent pipe flow

Swirling turbulent flow for a wide range of swirl numbers has been investigated in order to assess the interaction between the Dean vortices and the swirling motion. From a first impression of the mean velocity fields, depicted in figure 5, it is observed that the two symmetrical Dean vortices occupying the upper and lower side of the pipe are highly sensitive to perturbations. A slight increase in swirl intensity ( $S = 0.1$ ) breaks the symmetry of the Dean vortices as can be clearly observed. With increasing swirl rate the vortex core of the upper cell moves towards the center due to the solid-body-kind motion of the flow entering the pipe. At the same time, the lower cell gets attracted by the increasingly stronger upper cell and starts to deform significantly. As the swirl intensity increases further to  $S = 0.5$  the vortices continue to change location and the flow starts to take a more stabilized and structured form. Both structures can still be identified until a swirl number of  $S = 0.85$  where only one structure remains closer to the center of the pipe. At

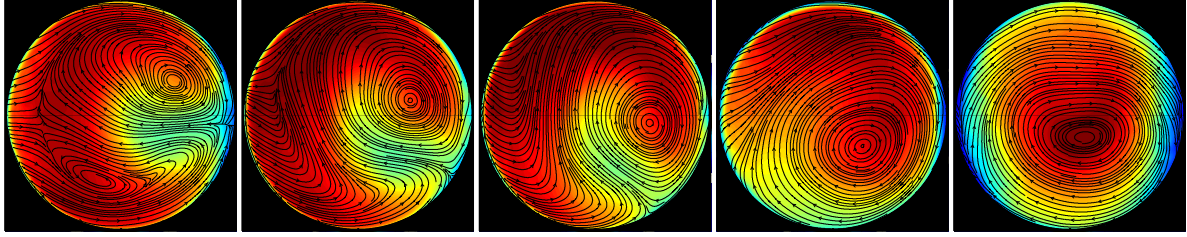


Figure 5: Mean velocity fields for different swirl numbers:  $S = 0.1, 0.3, 0.5, 0.85$  and  $1.2$  (from left to right). Streamwise velocity component scaled by the bulk velocity is shown as the background contour map while the secondary motion is plotted as the streamlines. The scaling and color coding is the same as in figure 2.

$S = 1.2$  a single vortex structure is positioned at the centre of the pipe and a well-structured and symmetric flow field is established. This description matches well with what has been found in the numerical study by Pruvost et al (2004) even though there exist differences between the two studies regarding the set up and flow parameters and therefore no direct comparison can be made.

In order to check whether there remain underlying large-scale vortical structures resembling Dean cells in the swirling flow field, the flow field has been decomposed by means of POD. Dealing with large scale structures, with the swirling motion being substantially more dominant than the Dean vortices (as can be seen in the mean velocity fields) POD was thought to be a useful tool in order to decompose the flow field and rank the obtained topo-modes (i.e. spatial modes) by energy content. It is expected, that the swirling motion—as the most energetic structure—will be the dominating feature in the 0-mode which represents the mean field and any other energetic vortical structure should be depicted in the following modes which represent the fluctuating part of the flow. The POD analysis was performed here on  $N_s = 1000$  snapshots with a temporal resolution of  $\Delta t_s = 1/1000$  s.

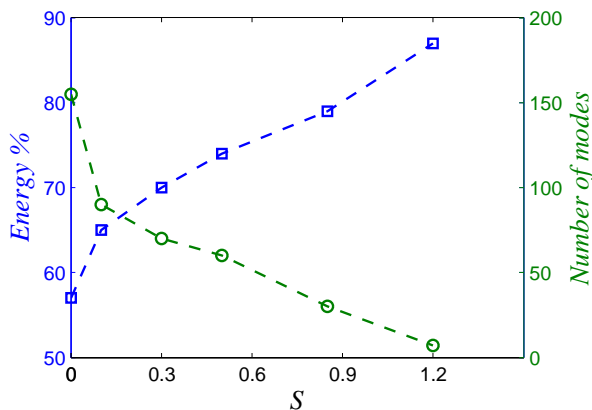


Figure 6: Relative energy content of the 0-mode ( $\square$ ) and number of modes needed to capture 90% of the total energy ( $\circ$ ) plotted against the swirl numbers  $S$ .

Figure 6 shows the relative energy content of the 0-mode (mean field) as a function of the swirl number  $S$ . Not unexpectedly, it can be seen that by increasing the swirl rate, the energy content of the respective 0-mode increases. The relative energy content for the  $S = 0.1$  case was 70%, rising up to almost 90% for the  $S = 1.2$  case. Moreover, the number of modes needed to reach 90% of the total energy was found to be significantly lower for the swirl dominated case, with a difference of more than 100 modes between the lowest and highest swirl number flow cases. That shows that the swirling motion contributes greatly to the total energy of the flow field, constituting also the most energetic structure.

The first topo-mode for all swirl cases is plotted in figure 7. Various vortical structures appear in all the cases, showing first of all, that vortical structures resembling to some degree Dean cells are embedded in the swirl dominated flow field. Those structures have a turbulent kinetic energy of 8 – 13% of the total, depending on the swirl case. Moreover in most of the cases the vortices have been rotated in reference to the plane of symmetry either in the clockwise or anti-clockwise direction.

## 4 Conclusions

Results from turbulent swirling flow at the exit of a  $90^\circ$  curved pipe have been presented for a wide range of swirl numbers. These experiments also constitute the first set of measurements in swirling turbulent flows through a pipe bend that provides the in-plane vortical structures. The effect of the swirling motion on the Dean vortices has been examined by combining TS-PIV data and POD analysis. POD has been used as a powerful tool to extract the most energetic structures in the flow field and succeeded to reveal both the unsteady behavior of the vortices under turbulent non-swirling flow conditions and the coherent structures underlying the swirling motion.

In particular, for the non-swirling turbulent flow case, similar behavior to that of the so-called “swirl-switching” phenomenon was captured by reconstructing the original snapshots with only few of the most

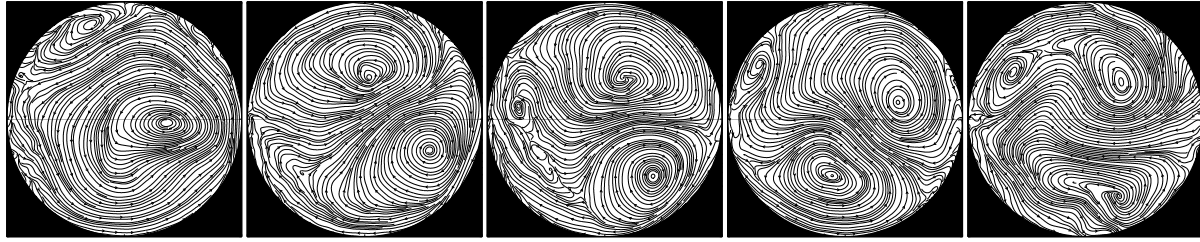


Figure 7: The first POD mode for the:  $S = 0.1, 0.3, 0.5, 0.85$  and  $1.2$  swirl flow cases from left to right with the secondary motion shown as streamlines.

energetic modes. The frequency at which the two vortices switch position alternatively could be determined by combining spectral analysis of the reconstructed time series and the first POD coefficient thereby confirming previous studies.

For the swirling turbulent flow it was shown that even for the lowest swirl number shown here, the stabilizing effect of the swirl is evident, moving the high speed fluid from the outer wall to the centre of the pipe. Axi-symmetry of the flow field is gradually achieved with increasing swirl number, as one of the Dean vortices with the same rotational direction as the imposed motion, drifts away and merges with the other vortex. This results in a single large scale motion located almost at the centre of the pipe for the swirl dominated flow field. The existence of underlying large-scale vortical structures in the swirling flow field was supported by their appearance in the most energetic POD modes.

The present work constitutes a preliminary investigation into the dynamics of turbulent swirling flow through pipe bends. POD has been deemed to be a powerful tool for the characterization of the large-scale vortical structures in such a flow and will be used for further analysis in the future. The data and results are further aimed to serve as a database for future analysis of the physics in the use of numerical simulations.

## Acknowledgments

This work is supported by CCGEx and the Linné Flow Centre. Prof. P. Henrik Alfredsson is acknowledged for comments on the manuscript. The authors would like to thank Tekn. Lic. Onofrio Semeraro for fruitful discussions on the POD analysis.

## References

Anwer, M. and So, R. M. C. (1993), Swirling turbulent flow through a curved pipe. Part 1: Effect of swirl and bend curvature, *Exp. Fluids*, Vol. 14, 85-86.

Brücker, C. (1998), A time-recording DPIV-Study of the swirl switching effect in a 90 bend flow, Proc. 8th Int. Symp. Flow Vis., 1-4 Sept., Sorrento (NA), Italy, 171.1-171.6.

Dean, W. R. (1927), Note on the motion of fluid in a curved pipe, *Phil.Mag.*, Vol. 4, 208-223.

Eustice, J. (1911), Experiments on stream-line motion in curved pipes, *Proc. Roy. Soc.*, Vol. 85, 119-131.

Kalpikli, A. (2012), Experimental study of turbulent flows through pipe bends, Licentiate thesis, KTH Mechanics, Stockholm, Sweden.

Kalpikli, A., Örlü, R. and Alfredsson, P. H. (2011), Dean vortices in turbulent flows: rocking or rolling?, *J. Vis.*, Vol.15, 37-38.

McConalogue, D. J. and Srivastava, R. S. (1968), Motion of a fluid in a curved tube, *Proc. Roy. Soc.*, Vol. 307, 37-53.

Meyer, K., Pedersen, J. M. and Özcan, O. (2007) A turbulent jet in crossflow analysed with proper orthogonal decomposition, *J. Fluid Mech.*, Vol. 583, 199.

Pruvost, J., Legrand, J. and Legentilhomme, P. (2004), Numerical investigation of bend and torus flows, part I: effect of swirl motion on flow structure in U-bend, *Chem. Eng. Sc.*, Vol. 59, 3345-3357.

Rütten, F., Schröder, W. and Meinke, M. (2005), Large-eddy simulation of low frequency oscillations of the Dean vortices in turbulent pipe bend flows, *Phys. Fluids*, Vol. 17, 035107.

Sakakibara, J. and Machida, N. (2012), Measurement of turbulent flow upstream and downstream of a circular pipe bend, *Phys. Fluids*, Vol. 24, 041702.

Sakakibara, J., Sonobe, R., Goto, H., Tezuka, H., Tada, H. and Tezuka, K. (2010), Stereo-PIV study of turbulent flow downstream of a bend in a round pipe, 14th Int. Symp. Flow Vis., 21-24 June, EXCO Daegu, Korea.

Sattarzadeh, S. S. (2011), Experimental study of complex pipe flows, Master thesis, KTH Mechanics, Stockholm, Sweden.

Sirovich, L. (1987), Turbulence and the dynamics of coherent structures. Part 1: Coherent structures, *Quart. Appl. Math.*, Vol. 45, 561-571.

Tunstall, M. J. and Harvey, J. K. (1968), On the effect of a sharp bend in a fully developed turbulent pipe-flow, *J. Fluid Mech.*, Vol. 34, 595-608.

Wieneke, B. (2005), Stereo-PIV using self-calibration on particle image, *Exp. Fluids*, Vol. 39, 267-280.